

Flux-dependent level attraction in double-dot Aharonov-Bohm interferometers

Björn Kubala and Jürgen König

Institut für Theoretische Festkörperphysik, Universität Karlsruhe, 76128 Karlsruhe, Germany

(Received 24 October 2001; published 28 May 2002)

We study electron transport through a closed Aharonov-Bohm interferometer containing two noninteracting single-level quantum dots. The quantum-dot levels are coupled to each other indirectly via the leads. We find that this coupling yields signatures of an effective *flux-dependent level attraction* in the linear conductance. Furthermore, we predict a *suppression of transport* when both levels are close to the Fermi level of the leads. The width of this anomaly is also flux dependent. We identify different regimes in which constructive interference of transmission through identical dots yields a signal that is 1, 2, or 4 times as large as the conductance through a single dot.

DOI: 10.1103/PhysRevB.65.245301

PACS number(s): 73.23.Hk, 73.63.Kv, 73.40.Gk

I. INTRODUCTION

The presence of quantum coherence in mesoscopic systems is detectable through interference experiments. Transport measurements through multiply connected geometries containing a quantum dot revealed oscillations of the conductance as a function of magnetic flux, i.e., Aharonov-Bohm (AB) oscillations,¹⁻⁴ provided that the phase coherence length is larger than the dimensions of the device. Differences between closed (two-terminal) AB interferometers^{1,4-9} and those with open geometries^{2,9} have been discussed, and Kondo correlations,^{3,10,11} the Fano effect,^{11,12} and the influence of Coulomb interaction on quantum coherence^{13,14} have been addressed.

More recently, an AB interferometer containing two quantum dots has been realized.¹⁵ The possibility to manipulate each of the quantum dots separately enlarges the dimension of the parameter space for the transport properties as compared to a single-dot AB interferometer, and the enterprise to experimentally explore the unknown territory has just begun. Theoretical work on transport through double-dot systems includes studies of resonant tunneling¹⁶ and cotunneling,^{17,18} as well as the prediction of asymmetric interference patterns,^{13,14} signatures of Kondo correlations,¹⁹ and a quantum phase transition²⁰ in the presence of strong Coulomb interactions. Spectral properties of double dots coupled to leads have been studied in Ref. 21.

In this paper, we study a simple model system of a closed double-dot AB interferometer, which can be solved exactly. Surprisingly, we find even for this model complex characteristic transport features such as signatures of a flux-dependent level attraction and an anomaly of suppressed transport, which can easily be manipulated by applied gate voltages and magnetic flux. Our aim is to provide a map with the most significant transport signals, which may serve as a guide for the ongoing and future experimental endeavor.

II. MODEL

We consider an AB geometry as depicted in Fig. 1. Two single-level quantum dots are coupled to leads, described by the standard tunnel Hamiltonian

$$H = \sum_{kr} \epsilon_{kr} a_{kr}^\dagger a_{kr} + \sum_{i=1,2} \epsilon_i c_i^\dagger c_i + \sum_{kri} (t_{ri} a_{kr}^\dagger c_i + \text{H.c.}), \quad (1)$$

where a_{kr}^\dagger and a_{kr} are the creation and annihilation operators for electrons with quantum number k in the left or right lead, $r=L$ or R , respectively, and c_i^\dagger and c_i are the Fermi operators for the states in dot $i=1,2$. The level energies in the dots (measured from the Fermi energy of the leads) are denoted by ϵ_1 and ϵ_2 . They can be varied by applied gate voltages. It is convenient for the following calculations to define the average level energy $\bar{\epsilon} = (\epsilon_1 + \epsilon_2)/2$ and the difference $\Delta\epsilon = \epsilon_2 - \epsilon_1$. We neglect the energy dependence of the tunnel matrix elements t_{ri} (Ref. 22) and assume a symmetric coupling strength $|t_{ri}| = |t|$. Due to tunneling, each dot level acquires a finite linewidth $\Gamma = \Gamma_L + \Gamma_R$ with $\Gamma_r = 2\pi|t|^2 N_r$, where N_r is the density of states in lead $r=L,R$. The magnetic flux is modeled by an AB phase attached to the tunnel matrix elements.²³ We choose a symmetric gauge such that $(t_{L1})^* = t_{L2} = (t_{R2})^* = t_{R1} = |t| \exp(i\varphi/4)$, with $\varphi \equiv 2\pi\Phi/\Phi_0$, and $\Phi_0 = h/e$ is the flux quantum.

In the above model there is no direct interaction (either Coulomb repulsion or tunnel coupling) between the two quantum dots. The levels are rather coupled indirectly to each other via the leads. Furthermore, since for each dot only one level supports the transport (for the level spacing being larger than bias voltage, linewidth, and temperature), no intradot Coulomb interaction terms enter the Hamiltonian.²⁴

The experimentally accessible quantity is the linear conductance $G^{\text{lin}} = (\partial I / \partial V)|_{V=0}$, which is related to the transmission $T(\omega)$ for an electron with energy ω by

$$G^{\text{lin}} = -\frac{e^2}{h} \int d\omega T(\omega) f'(\omega), \quad (2)$$

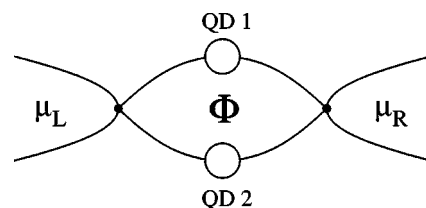


FIG. 1. Double-dot Aharonov-Bohm interferometer.

where $f'(\omega)$ is the derivative of the Fermi-Dirac distribution function.

III. EXACT TRANSMISSION FORMULA

Since Eq. (1) describes a model of noninteracting electrons, the total transmission $T(\omega)$ can be expressed²⁵ as

$$T(\omega) = \text{tr}\{\mathbf{G}^a(\omega)\mathbf{\Gamma}^R\mathbf{G}^r(\omega)\mathbf{\Gamma}^L\}, \quad (3)$$

where $\mathbf{G}^{r/a}(\omega)$ is the matrix of retarded/advanced dot Green's functions, and $\mathbf{\Gamma}^{L/R}$ describes the coupling to the left/right lead. The matrix elements for the retarded Green's functions are defined in time space as $G_{ij}^r(t) = -i\Theta(t) \times \langle\{c_i(t), c_j^\dagger(0)\}\rangle$. The 2×2 matrix structure accounts for the two quantum dots (we set $\hbar = 1$ from now on). The tunnel coupling is described by

$$\mathbf{\Gamma}^L = (\Gamma/2) \begin{pmatrix} 1 & \exp(i\varphi/2) \\ \exp(-i\varphi/2) & 1 \end{pmatrix}$$

and $\mathbf{\Gamma}^R = (\mathbf{\Gamma}^L)^*$.

We obtain the exact equilibrium Green's functions by employing an equation-of-motion approach. Briefly, this method consists of using the time evolution $i\partial_t c_i = [c_i, H]$ to relate the time derivative $\partial_t G_{ij}^r(t)$ to $G_{ij}^r(t)$ and new Green's functions involving one dot- and one lead-electron operator. We repeat this for these newly generated Green's functions until we get a closed set of equations. Eventually, we obtain the solution

$$\mathbf{G}^r(\omega) = \begin{pmatrix} \omega - \epsilon_1 + i\frac{\Gamma}{2} & i\frac{\Gamma}{2} \cos\frac{\varphi}{2} \\ i\frac{\Gamma}{2} \cos\frac{\varphi}{2} & \omega - \epsilon_2 + i\frac{\Gamma}{2} \end{pmatrix}^{-1} \quad (4)$$

and for $\mathbf{G}^a(\omega)$ the complex conjugate. Inserting this result into Eq. (3) leads to the total transmission

$$T(\omega) = \frac{\Gamma^2 \left[(\omega - \bar{\epsilon})^2 \cos^2 \frac{\varphi}{2} + \left(\frac{\Delta\epsilon}{2} \right)^2 \sin^2 \frac{\varphi}{2} \right]}{\left[(\omega - \bar{\epsilon})^2 - \left(\frac{\Delta\epsilon}{2} \right)^2 - \left(\frac{\Gamma}{2} \right)^2 \sin^2 \frac{\varphi}{2} \right]^2 + (\omega - \bar{\epsilon})^2 \Gamma^2} \quad (5)$$

This is the central and most general result of this paper.

IV. LEVEL ATTRACTION AND SUPPRESSED TRANSPORT

We analyze the transport as a function of the bare energy-level positions (or, equivalently, the gate voltages). At low temperature, the linear conductance is just e^2/h times the transmission $T(\omega=0)$ of incoming electrons at the Fermi energy. The latter is shown in Fig. 2 for finite magnetic flux (we arbitrarily choose the value $\varphi = 2\pi/5$). We find that there are two striking features: lines of full transmission $T = 1$ and a sharp anomaly of suppressed transport around $\epsilon_1 = \epsilon_2 = 0$.

The lines of full transmission $T = 1$ form hyperbolas $\bar{\epsilon}^2$

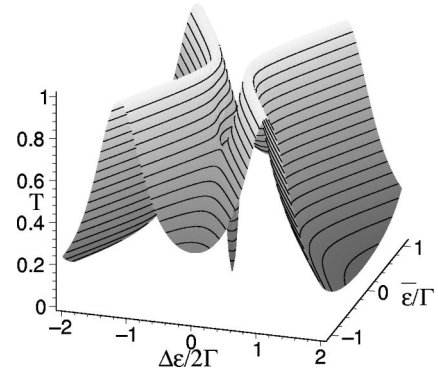


FIG. 2. Transmission $T(\omega=0)$ as a function of the average $\bar{\epsilon}$ and difference $\Delta\epsilon$ of the dot level energies for $\varphi = 2\pi/5$.

$-(\Delta\epsilon/2)^2 = -(\Gamma/2)^2 \sin^2(\varphi/2)$; see thick solid lines in Fig. 3. Intuitively, one could interpret the incidence of full transmission as resonance of *renormalized* dot levels with the Fermi level of the leads. Starting from bare levels ϵ_1, ϵ_2 , we find the renormalized level positions as the ω values that satisfy $T(\omega) = 1$. Following this picture, we find no renormalization as long as the bare level energies are well separated, $|\Delta\epsilon| \gg \Gamma |\sin(\varphi/2)|$, but an effective *flux-dependent level attraction* otherwise. This leads to lines of $T(\omega=0) = 1$ in the $\epsilon_1 \cdot \epsilon_2 < 0$ region of Fig. 3 (as opposed to lines in the $\epsilon_1 \cdot \epsilon_2 > 0$ region, which would indicate level *repulsion*). The strength of the level attraction depends on the AB phase. The maximum is achieved for odd-integer values of φ/π (see dashed lines separating white and shaded regions in Fig. 3 for full transmission), and level attraction vanishes at $\varphi = 0$; see diagonals (dotted lines). We remark that there is a subtlety in interpreting full transmission as a resonance condition. The dot structure probed by transport may differ from the real one obtained from direct spectroscopy since different linear combinations of the bare dot levels couple differently strong to the leads. In fact, it has been shown²¹ that in the absence of magnetic flux our model shows a level attraction with the real level positions being defined by the maximum

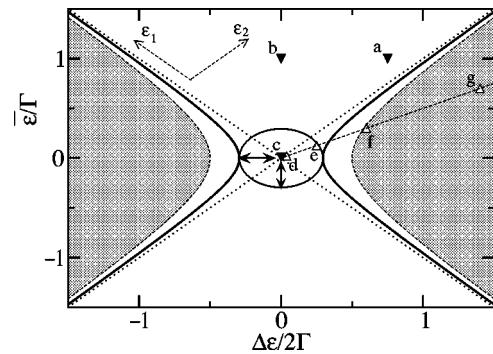


FIG. 3. Sketch of the significant features of the transmission for $\varphi = 2\pi/5$. Thick solid lines (hyperbolas) denote full transmission, $T = 1$. Dotted lines (diagonals) indicate the lines of full transmission for the case $\varphi = 0$. The circle in the middle sketches the boundary of the anomaly of suppressed transmission. Its half width (arrows) is $|\sin(\varphi/2)|/2$. In the white and shaded regions, AB oscillations show a minimum and a maximum at flux $\varphi = \pi$, respectively (see Fig. 4).

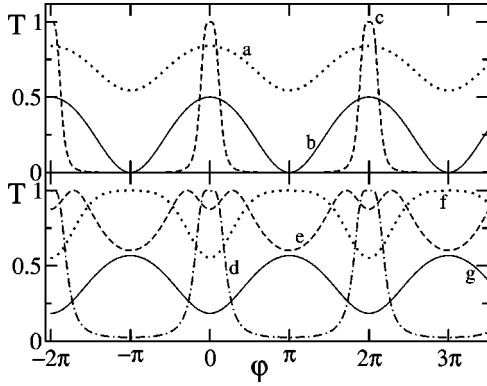


FIG. 4. AB oscillations for different values of $(\Delta\epsilon/2\Gamma, \bar{\epsilon}/\Gamma)$ as indicated in Fig. 3. *a*: (0.75,1), *b*: (0,1), *c*: (0,0.01), *d*: (0.04,0.02), *e*: (0.25,0.125), *f*: (0.6,0.3), and *g*: (1.4,0.7).

of the spectral density. In contrast, the level positions defined by the transport signal as discussed in this paper are not renormalized at $\varphi=0$.

Around the point $\bar{\epsilon}=\Delta\epsilon=0$ there is a sharp anomaly of suppressed transmission [with $T=0$ at $\bar{\epsilon}=\Delta\epsilon=0$]. The width of this dip is $|\sin(\varphi/2)|$, as it is bound by the lines of full transmission on the $\Delta\epsilon/(2\Gamma)$ axis and by saddle points (with height $T=\cos^2(\varphi/2)$) on the $\bar{\epsilon}/\Gamma$ axis (see Figs. 2 and 3). For the special case $\Delta\epsilon=0$ this dip was already found in Ref. 16. We emphasize that both the anomaly of suppressed transmission and the effective level attraction are *not* captured by a first- or second-order perturbation expansion in Γ .

V. AB OSCILLATIONS

We now discuss the shape of the AB oscillations, i.e., oscillations of the transmission as a function of magnetic flux for fixed level positions ϵ_1 and ϵ_2 (see Fig. 4). Two features will be emphasized: the evolution of sharp peaks close to the anomaly of suppressed transmission and a maximum-to-minimum transition of the transmission around the AB phase $\varphi=\pi$.

Away from the anomaly in the center, the oscillations are sinusoidal (curves *a*, *b*, and *g* in Fig. 4). When entering the region of the anomaly in the center of the diagram in Fig. 3, higher-harmonic contributions become important (see curves *e* and *f*). These correspond to paths through the AB geometry with higher winding number around the enclosed flux (the phase coherence length has to be longer than these paths). Close to the center, sharp peaks around AB-phase values $0, \pm 2\pi, \pm 4\pi, \dots$ result (curves *c* and *d*). This opens the possibility to manipulate transport in a nontrivial way by varying the magnetic field. *The sensitivity of this dependence is determined by the gate voltages of the quantum dots.*

The behavior of the transmission near flux values $\pm\pi, \pm 3\pi, \dots$ underpins the notion of an effective flux dependent level attraction. In the regime indicated by the white region in Fig. 3, the AB oscillations show a minimum as a function of φ , while in the shaded region a maximum occurs. This is consistent with interpreting the lines of full transmission as the renormalized energy levels being in resonance

with the Fermi level, as we did above: In the shaded region, the two *renormalized* dot levels are on opposite sides of the Fermi energy while they are on the same side in the white region. If a dot level is lying above the Fermi energy, particle-like processes will dominate transport through that dot, while hole-like processes dominate in the opposite case. The corresponding transmission phases differ by π which explains the maximum to minimum transition.

VI. FANO LINE SHAPES

Interference between resonant transport through a single level and a continuous background channel yields asymmetric line shape for the conductance as a function of the level position, the well-known Fano effect.²⁶ Within our model we can simulate such a situation by keeping one energy level, say ϵ_2 , fixed and varying the other one ϵ_1 . Transport through quantum dot 2 provides then the “background channel” with transmission $T_b = (\Gamma/2)^2 / [\epsilon_2^2 + (\Gamma/2)^2]$. After defining $e \equiv -[\epsilon_1 + \text{Re} \Sigma(0)] / \text{Im} \Sigma(0)$ with $G_{11}^f(\omega) = 1 / [\omega - \epsilon_1 - \Sigma(\omega)]$ obtained by Eq. (4) and the Fano parameter $q \equiv (2\epsilon_2/\Gamma)[-1 + (2 - T_b)\cos^2(\varphi/2)] / [1 - T_b\cos^2(\varphi/2)]$, we find the generalized Fano form

$$T = T_b \frac{(e+q)^2}{e^2+1} + \frac{A \sin^2 \varphi}{e^2+1} \quad (6)$$

at $\omega=0$, with $A = (1 - T_b) / [1 - T_b \cos^2(\varphi/2)]^2$. For dot level 2 tuned far away from resonance, $|\epsilon_2| \gg \Gamma/2$, A approaches unity.²⁷

VII. DESTRUCTIVE AND CONSTRUCTIVE INTERFERENCE

The textbook example for quantum interference effects is the two-slit experiment. The standard way to demonstrate destructive and constructive interference is to consider a setup where the moduli of the transmission amplitudes through either slit are identical, $|t_1|=|t_2|=|t|$, and to tune the relative phase such that the total transmission probability $|t_1+t_2|^2$ becomes extremal, i.e., 0 for destructive and $4|t|^2$ for constructive interference. There is, however, a principal difference between this two-slit setup and the double-dot AB interferometer we study. In the former one only a fraction of the emitted particles reach the detector while most of them are scattered to the periphery. The latter has a closed geometry, and all incoming electron must either arrive at the drain or be backscattered to the source. Therefore, we can ask the question whether destructive and constructive interference will still emerge in our model system.

To make the analogy to the two-slit setup as close as possible, we consider equal level energies $\epsilon_1 = \epsilon_2 = \epsilon$. It is easy to see from Eq. (5) that destructive interference, $T=0$, is achieved for φ being an odd multiple of π , which proves that in our model the transport is fully coherent for all temperatures and coupling strengths.²⁸

The situation $\varphi=0$ corresponds to the constructive-interference scenario in the two-slit experiment. At $\varphi=0$ (and $\Delta\epsilon=0$) the transmission through the double-dot AB

interferometer has Breit-Wigner form $T_{2 \text{ dot}}(\omega) = \Gamma^2 / [(\omega - \epsilon)^2 + \Gamma^2]$, but with a level width twice as large as for a single dot, $T_{1 \text{ dot}}(\omega) = (\Gamma/2)^2 / [(\omega - \epsilon)^2 + (\Gamma/2)^2]$. This can be easily understood by writing the Hamiltonian in terms of symmetric and antisymmetric combinations of the dot levels to see that the antisymmetric combination decouples, whereas the symmetric combination acquires an increased coupling strength, $t \rightarrow \sqrt{2}t$.

It follows that at low temperature and at resonance $|\epsilon|, k_B T \ll \Gamma$, the linear conductance through the double-dot system is equal to that through a single dot $G_{1 \text{ dot}}^{\text{lin}} = e^2/h$ in the absence of the other arm of the interferometer, $G_{2 \text{ dot}}^{\text{lin}}/G_{1 \text{ dot}}^{\text{lin}} = 1$.

At high temperature, $|\epsilon|, \Gamma \ll k_B T$, the conductance is dominated by contributions in first order in Γ , and subsequently, we obtain $G_{2 \text{ dot}}^{\text{lin}}/G_{1 \text{ dot}}^{\text{lin}} = 2$ (see also Refs. 13 and 14).

It is only in the regime $\Gamma, k_B T \ll |\epsilon|$ (the so-called cotunneling regime, in which transport is of order Γ^2) that the ratio $G_{2 \text{ dot}}^{\text{lin}}/G_{1 \text{ dot}}^{\text{lin}} = 4$ reaches the value as for constructive interference in the two-slit experiment.

VIII. SUMMARY

We studied transport through an Aharonov-Bohm interferometer containing two noninteracting, single-level quantum dots. Based on the derivation of an exact expression for the total transmission we found signatures of a flux-dependent level attraction and an anomaly of suppressed transport. We analyzed the form of AB oscillations in different regions of the parameter space, and found the evolution of sharp peaks near the anomaly of suppressed transport and a maximum-to-minimum transition of the AB signal around $\varphi = \pi$. Regimes where constructive interference through identical dots yields a transmission that is 1, 2, or 4 as large as that through a single quantum dot were identified.

ACKNOWLEDGMENTS

We acknowledge helpful discussions with D. Boese, Y. Gefen, Y. Imry, H. Schoeller, and G. Schön. This work was supported by the Deutsche Forschungsgemeinschaft through the Emmy-Noether program and the Center for Functional Nanostructures.

-
- ¹A. Yacoby, M. Heiblum, D. Mahalu, and H. Shtrikman, *Phys. Rev. Lett.* **74**, 4047 (1995).
- ²R. Schuster, E. Buks, M. Heiblum, D. Mahalu, V. Umansky, and H. Shtrikman, *Nature (London)* **385**, 417 (1997).
- ³Y. Ji, M. Heiblum, D. Sprinzak, D. Mahalu, and H. Shtrikman, *Science* **290**, 779 (2000); Y. Ji, M. Heiblum, and H. Shtrikman, *Phys. Rev. Lett.* **88**, 076 601 (2002).
- ⁴W. G. van der Wiel, S. De Franceschi, T. Fujisawa, J. M. Elzerman, S. Tarucha, and L. P. Kouwenhoven, *Science* **289**, 2105 (2000).
- ⁵A. L. Yeyati and M. Büttiker, *Phys. Rev. B* **52**, R14 360 (1995).
- ⁶G. Hackenbroich and H. A. Weidenmüller, *Phys. Rev. Lett.* **76**, 110 (1996).
- ⁷C. Bruder, R. Fazio, and H. Schoeller, *Phys. Rev. Lett.* **76**, 114 (1996).
- ⁸R. Baltin and Y. Gefen, *Phys. Rev. Lett.* **83**, 5094 (1999).
- ⁹O. Entin-Wohlman, A. Aharony, Y. Imry, Y. Levinson, and A. Schiller, *Phys. Rev. Lett.* **88**, 166801 (2002).
- ¹⁰U. Gerland, J. v. Delft, T. A. Costi, and Y. Oreg, *Phys. Rev. Lett.* **84**, 3710 (2000).
- ¹¹W. Hofstetter, J. König, and H. Schoeller, *Phys. Rev. Lett.* **87**, 156 803 (2001).
- ¹²O. Entin-Wohlman, A. Aharony, Y. Imry, and Y. Levinson, *J. Low Temp. Phys.* **126**, 1251 (2002).
- ¹³J. König and Y. Gefen, *Phys. Rev. Lett.* **86**, 3855 (2001).
- ¹⁴J. König and Y. Gefen, *Phys. Rev. B* **65**, 045 316 (2002).
- ¹⁵A. W. Holleitner, C. R. Decker, H. Qin, K. Eberl, and R. H. Blick, *Phys. Rev. Lett.* **87**, 256 802 (2001).
- ¹⁶T. V. Shahbazyan and M. E. Raikh, *Phys. Rev. B* **49**, 17 123 (1994).
- ¹⁷H. Aker, *Phys. Rev. B* **47**, 6835 (1993).
- ¹⁸D. Loss and E. V. Sukhorukov, *Phys. Rev. Lett.* **84**, 1035 (2000).
- ¹⁹D. Boese, W. Hofstetter, and H. Schoeller, *Phys. Rev. B* **64**, 125 309 (2001).
- ²⁰W. Hofstetter and H. Schoeller, *Phys. Rev. Lett.* **88**, 016803 (2002).
- ²¹J. König, Y. Gefen, and G. Schön, *Phys. Rev. Lett.* **81**, 4468 (1998).
- ²²This widely used approximation works since only lead states close to the Fermi energy participate in transport.
- ²³A magnetic-field dependence of ϵ_1 and ϵ_2 is unimportant for the subsequent discussion. It would just shift the curves shown in Figs. 2 and 3, and the corrections to the AB oscillations shown in Fig. 4 would be negligible as long as the area of each quantum dot is small as compared to the area enclosed by the interferometer arms.
- ²⁴Such terms are absent not only in devices, in which Coulomb interaction within each dot can be neglected, but also when spin degeneracy is lifted in a strong Zeeman field or in an antiferromagnetic sample.
- ²⁵Y. Meir and N. Wingreen, *Phys. Rev. Lett.* **68**, 2512 (1992).
- ²⁶U. Fano, *Phys. Rev.* **124**, 1866 (1961).
- ²⁷We note that Eq. (6) and the definition of the Fano parameter q are identical to those for a closed single-dot AB interferometer [see Eqs. (4) and (5) of Ref. 11] but with a renormalized flux $\tilde{\varphi}$ defined by $\sin^2 \tilde{\varphi} = A \sin^2 \varphi$.
- ²⁸The apparent contradiction to a naive sequential-tunneling picture which yields incoherent transport at high temperatures has been addressed in Refs. 13 and 14.